

## Transient Second Harmonic Generation from Oxazine Dyes at the Air/Water Interface

Daniel A. Steinhurst,<sup>†</sup> Andrew P. Baronavski,<sup>‡</sup> and Jeffrey C. Owrutsky\*

Code 6111, U.S. Naval Research Laboratory, Washington, DC 20375-5342

Received: August 30, 2001; In Final Form: January 7, 2002

Ultrafast surface second harmonic generation (SHG) studies are reported for several oxazine dyes at the air/water interface. As we demonstrated previously [*J. Phys. Chem. B* **2001**, *105*, 3062] in our steady-state SHG studies of aqueous oxazine dye solutions, the SHG signals are almost entirely due to dimers. The transient SHG recovery is biexponential with time constants of 4–8 ps and 22–44 ps depending on the dye and the solution composition. The SHG recovery is one-photon resonant and is attributed to two parallel ground state recovery mechanisms. Transient absorption signals were also measured for bulk dye solutions of water and methanol, and the results indicate a fast (2 ps) solvation dynamics component as well as a longer component due to the excited state lifetime (>400 ps) of the dye monomer. Therefore, both decay times observed for the dyes at the surface are different than what is seen for bulk solution, and they resemble what has been previously reported for dye aggregates.

## Introduction

Aggregates of organic molecules, which have been investigated to the greatest extent for dyes, play a significant role in chemical processes that occur in photography, biological systems, and for materials and devices involving optical interactions such as nonlinear optical materials and light-harvesting devices. As an example of the latter, dyes are used to cap semiconductors to extend the wavelength coverage for photovoltaic cells,<sup>1–6</sup> and recent studies have demonstrated that electron-transfer rates are different for monomer and aggregate molecules.<sup>7</sup>

We report one of the first ultrafast studies of dye aggregates at the air/water interface. There have been previous ultrafast studies of monomeric species at the air/water interface (and other air/liquid interfaces) as well as investigations of aggregates at air/solid and liquid/solid interfaces, many of the latter involving silica. In the former case, Eisenthal and co-workers<sup>8</sup> have pioneered the study of interface ultrafast dynamics using time-resolved second harmonic generation to investigate phenomena such as rotational reorientation,<sup>9</sup> photoisomerization,<sup>10</sup> and solvation dynamics.<sup>11,12</sup> Similar studies have also been reported by Girault and co-workers, who investigated rotational diffusion of eosin B.<sup>13</sup> Considerably less has been reported on the dynamics of aggregates in bulk solution<sup>14,15</sup> than at air/solid and liquid/solid interfaces.<sup>1–5,16–20</sup>

Many cationic dyes form H-aggregate dimers more readily in aqueous solution and at solid interfaces than in organic solvents.<sup>1–5,14,16–21</sup> The exciton theory of dipole–dipole coupling can be used to relate the distance and relative orientation of monomeric dye molecules within the aggregate to the electronic structure, the resulting spectral shifts, and the transition moments of the aggregate.<sup>22–25</sup> For a dimer composed of two monomer units with parallel transition moments, the first excited singlet energy levels of the dimer are split into two

levels, one lower ( $S^-$ ) and one higher ( $S^+$ ) in energy than the first excited singlet state of the separated monomers. The allowed transitions and observed dimer band positions relative to the monomer depend on  $\Theta$ , the angle between the center of separation and the monomer transition moments. For “sandwich-type” H-aggregates,  $54.7^\circ \leq \Theta \leq 90^\circ$  (at  $\Theta = 90^\circ$ , the monomer dipole moments are aligned parallel), only transitions to the  $S^+$  energy level are allowed with the resulting absorption band blue shifted from the monomer. For J-aggregates,  $\Theta < 54.7^\circ$  (at  $0^\circ$ , the monomer dipole moments are aligned end-to-end), only transitions to the  $S^-$  energy level are allowed and the absorption band is red shifted.<sup>22–25</sup> For H-aggregates there is rapid internal conversion (IC) of population in the  $S^+$  energy level to the  $S^-$  singlet level, such that the fluorescence is greatly reduced as reported for cresyl violet.<sup>17,26</sup>

Time-resolved studies on aggregates often reveal a new decay on the 20–250 ps scale typically not observed in the bulk monomeric solution that has proven to be a challenge to assign. Anfinrud et al.<sup>17</sup> found no conclusive evidence of cresyl violet (CV) dimer time-resolved fluorescence for CV adsorbed on silica. Clark et al.<sup>14</sup> used transient absorption (TA) to study rhodamine B (RB) and found unique RB monomer and dimer excited-state lifetimes of 1.6 ns and 100 ps, respectively. Polarization-resolved measurements of the anisotropy decay indicated that the rotational diffusion time was longer than the fluorescence lifetime for the faster decay, which was interpreted as evidence that the species monitored was large, i.e., a dimer. Several cyanine dyes studied by Khairutdinov and Serpone<sup>15</sup> exhibited excited-state lifetimes ranging from 126 to 270 ps depending on the type of aggregate formed by each dye and the solution composition. They suggested that nonradiative relaxation from the excited state leads to heating of the aggregate and the local solvent shell. This heating could then result in deaggregation, shorter excited state lifetimes, and additionally decreased charge injection efficiency for light harvesting applications. The dynamics of several dye aggregates adsorbed on silica surfaces have been studied by Meech and co-workers. In the case of rhodamine 110 (R110),<sup>20</sup> the formation of dimers and larger aggregates was invoked to interpret the observed

\* Corresponding author. E-mail: jeff.owrutsky@nrl.navy.mil. Fax: (202) 404-8119.

<sup>†</sup> NRL—NRC Research Associate. E-mail: das@ccs.nrl.navy.mil.

<sup>‡</sup> E-mail: andrew.baronavski@nrl.navy.mil.

decays. The orientation of these aggregates at the surface was found to be independent of coverage below a monolayer. They made similar findings for rhodamine 6G (R6G)<sup>18</sup> and malachite green (MG)<sup>19</sup> on silica surfaces. In addition to the present study, Kamat and co-workers<sup>1–5</sup> and Nasr and Hotchandani<sup>6</sup> have studied the aggregates of several dyes including the oxazines in aqueous solution and on nanoparticles ( $\text{SiO}_2$ ,  $\text{SnO}_2$ ). They found that aggregates formed on  $\text{SiO}_2$  particles exhibited excited-state decay times of 2.2 to 250 ps depending on the dye. In all cases except R6G, aggregates formed on  $\text{SnO}_2$  particles exhibited a new longer time in addition to the time observed on  $\text{SiO}_2$ . These times, ranging from 12 ps to 3 ns, were interpreted as being due to various charge injection processes between the aggregate dication and the semiconductor particle. Grätzel and co-workers reported similar findings for coumarin 343 on  $\text{TiO}_2$  nanoparticles; they measured an excited-state lifetime of 350 fs on  $\text{TiO}_2$ , whereas no decay was observed in a methanol solution.<sup>27</sup>

As first observed by Levinger et al.<sup>21</sup> for IR125 and then in our recent study of oxazine dyes,<sup>28</sup> it appears that for dyes that are sparingly soluble in water, dimers form preferentially at the air/water interface. In the former case, Levinger et al.<sup>21</sup> attributed the surface second harmonic generation (SHG) spectra to dimers because they were similar to bulk spectra of the dye solutions with salt ( $\text{CaCl}_2$ ) added, which induces dimer formation. In our case, we determined that the SHG signals for the oxazine dyes at the air/water interface were due to dimers based on the signal dependence on solution composition as well as on the SHG spectra and adsorption curves. Polarization dependence studies indicated that the dimer orientation does not vary with concentration or addition of salt so that the signal changes observed as a function of solution composition were due to surface concentration changes.

We report an ultrafast study of the oxazine dyes Nile blue (NB), CV, and oxazine 720 (OX720) at the air/water interface by single-color, time-resolved second harmonic generation (TSHG). Bulk dye solutions of water and methanol were also studied by transient absorption/gain (TA/TG) measurements. The TA/TG signals are consistent with solvation times and excited state lifetimes reported in the literature. The TSHG signals exhibit a different response than those from the bulk solutions; the initial SHG reduction recovers biexponentially with intermediate time constants (between those for the solvation times and those for the excited-state lifetimes). Since the SHG probe is one-photon resonant with the incident pulse wavelength, the transients are attributed to ground-state recovery (GSR) of the dimers.

## Experimental Section

The details of the SHG experimental setup have been discussed elsewhere<sup>28</sup> and will be outlined only briefly here. The femtosecond laser system used has been described previously<sup>29</sup> with the addition of a home-built optical parametric amplifier (OPA) which is described below. The perchlorate salts of OX720, CV, and NB were obtained from Exciton and used without further purification. All solutions were prepared using triply deionized water, and reagent grade lithium chloride ( $\text{LiCl}$ ) was added where noted, 0.01 M for NB and 0.1 M for CV and OX720. Solutions with dye concentrations between  $7.5 \times 10^{-5}$  and  $3.0 \times 10^{-4}$  M were prepared by sonicating a saturated solution for 30 min, filtering, and diluting. Solution concentrations were determined based on their absorption spectra.

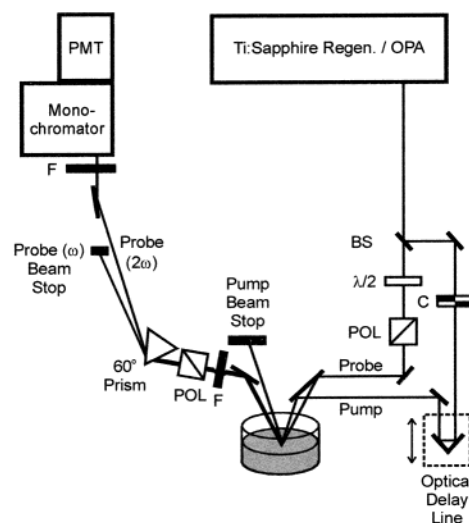


**Figure 1.** Schematic of experimental apparatus for single-color, visible pump-SHG probe transient measurements. See text for definitions of labels within figure. Some optical elements are not shown for clarity. Unmarked elements are mirrors.

Laser pulses tunable near 600 nm were generated with an OPA which produces 400 fs pulse width,  $\leq 30 \mu\text{J}$  pulses operating at a one kilohertz repetition rate. The OPA is pumped by the frequency-doubled output (400 nm) of a regeneratively amplified Ti:sapphire laser system.<sup>29</sup> Approximately  $6 \mu\text{J}$  of the pulse energy is used to generate continuum in a 3.38 mm thick piece of sapphire. A small fraction (10%) of the continuum pulse is split off and used as the probe for the TA/TG measurements. The rest of the continuum pulse is used to seed the OPA. Most of the fundamental (800  $\mu\text{J}$ ) is frequency-doubled in a BBO crystal (2 mm, type I,  $\theta = 29^\circ$ ) to produce a 100  $\mu\text{J}$ , 400 nm beam. After filtering out the fundamental, about 20  $\mu\text{J}$  of this beam is overlapped spatially and temporally with the continuum pulse in the OPA first stage crystal (BBO, 2 mm, type I,  $\theta = 29^\circ$ ) with a 100 mm focal length lens. The signal and idler beams are overlapped collinearly with the remaining 80  $\mu\text{J}$  of the 400 nm and focused with a 200 mm focal length lens into the second stage OPA crystal (BBO, 4 mm, type I,  $\theta = 29^\circ$ ). A color glass filter is used to remove the remaining 400 nm from the OPA output, yielding pulses that are tunable in the range 560–700 nm with a peak pulse energy of 20–30  $\mu\text{J}$  and typical bandwidths of 10–20 nm. The instrument function is about 350 fs as determined by cross-correlation using a 0.2 mm thick type I BBO crystal.

For the bulk experiments, OPA pump and continuum probe pulses are focused at a small angle by a 100 mm focal length lens into a 0.2 mm thick quartz cell containing the dye solution. The probe beam is attenuated with neutral density filters after the sample to avoid saturation of the silicon photodiode detector. For the surface SHG experiments (see Figure 1), the OPA pulses are split into two beams by a 50% visible beam splitter (BS) with approximately equal energy (10  $\mu\text{J}$  each) for the pump and probe beams. They are directed above the sample with a periscope and focused onto the air/water interface with a 100 mm focal length lens such that they are incident at the surface approximately 1 cm from the focal spots. The beams are offset laterally so that they are not collinear, and the angle between them at the sample is about  $6^\circ$ . The incident angle is  $33^\circ$  with respect to the surface normal. Approximately 30 mL of the sample is placed in a polystyrene dish and stirred to produce a fresh surface for each laser pulse. The reflected pump beam is

blocked with an iris. The reflected probe fundamental and the second harmonic beam generated by it are collected by a 100 mm focal length lens and redirected parallel to the laser table at the original beam height by a second periscope. The fundamental and harmonic frequencies are dispersed by a fused silica (FS) 60° prism and directed into a 0.25 m monochromator (Jarrell-Ash) and the output is detected on a photomultiplier tube (PMT, Hamamatsu R446). Both the monochromator and additional color glass filters (F) were used to verify that the measured signal was an SHG signal and not bulk fluorescence.

The probe beam, which is the fundamental for the TA experiments and the SHG for the surface experiments, is collected and the resulting detector output is sent to a lock-in amplifier (LIA, SRS 530). For both the TA and the surface SHG experiments, the pump beam is modulated at half the laser repetition rate by a mechanical chopper (C). A computer program controls the delay line for the probe pulse and collects the LIA output during each scan as a function of delay time. The electric field polarizations of both the pump and the probe pulses are vertical (*p*-polarized) unless otherwise indicated. The polarization of either the pump or probe beams can be rotated with the addition of a half-wave plate ( $\lambda/2$ ) and polarizing beam splitter cubes (POL) as shown in Figure 1.

## Results

**Overview.** Single-color TSHG measurements at the air/water interface are presented for aqueous solutions of OX720, CV, and NB. A small amount of salt (LiCl) was added to enhance the degree of aggregation and to increase the SHG signal intensity. Results were also obtained for aqueous NB solution without salt. To provide a basis for comparison with the TSHG results, TA/TG measurements were carried out for bulk aqueous and methanolic solutions of the same dyes using excitation near 600 nm and a range of probe wavelengths (480–700 nm). The surface results are compared with those from the bulk measurements and with those previously reported in studies of aggregates, particularly at interfaces. Possible interpretations for the observed TSHG signals are then discussed.

**Bulk TA/TG Results.** The TA/TG measurements of the bulk dye solutions were carried out under experimental conditions that would favor detecting the bulk transient response of the aggregates, which are clearly evident in the steady-state absorption spectra. Specifically, the bulk measurements were carried out for aqueous solutions with high concentrations of dye ( $[M_0] = 1\text{--}5 \times 10^{-4}$  M), for which the dimer and monomer absorptions are comparable, and using short wavelength excitation (580 nm) to excite near the aggregate band position. Bulk methanol solutions were also investigated as a way to identify any unique aggregate dynamics in the aqueous solutions. Both the aqueous and methanolic solutions yield transient absorption responses that can be described in terms of well-known dynamical processes. The response is consistent with a fast, probe wavelength-dependent component (2 ps) due to the time-dependent Stokes shift and characteristic of solvation dynamics and a longer (persistent on our time scale) component consistent with the known excited-state lifetimes in water. The 2 ps decay time we measure for the oxazines in water and the wavelength dependence of the fast decay are consistent with a time-dependent Stokes shift, which is reported to be 1.2 ps for water.<sup>30</sup> Numerous fluorescence studies have clearly established the fluorescence lifetimes of the dye monomers in water: 420 ps for NB,<sup>31</sup> 3.2–3.4 ns for CV,<sup>17</sup> and 1.79 ns for OX720.<sup>31</sup> These times are well beyond the time scale of our measurements and

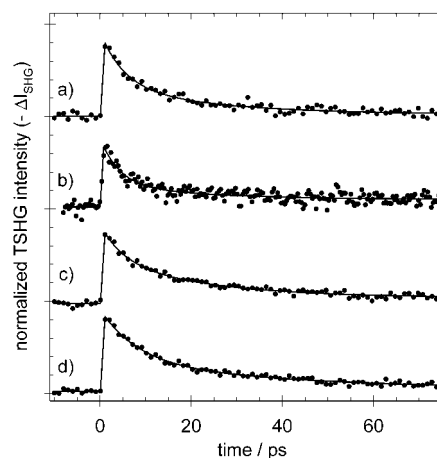


**Figure 2.** Normalized TSHG signal intensity (570 nm pump/570 nm probe) scans for aqueous/LiCl solutions of (a) oxazine 720, (b) cresyl violet, (c) Nile blue, and (d) an aqueous solution of Nile blue without LiCl. The solid lines represent biexponential fits to the data. The numerical results of the fits are found in Table 1.

will therefore appear as persistent components. Two important results of the bulk transient studies are that no intermediate (5–100 ps) decay is observed and there is no evidence of unique dynamics arising from aggregates in the bulk solution. The wavelength dependence of the long time signal is consistent with the transient solution spectra previously reported for CV by Liu and Kamat<sup>1</sup> and for NB by Nasr and Hotchandani.<sup>6</sup>

No detectable dye aggregation occurs in methanolic dye solutions, yet transient absorption measurements yield results similar to those for aqueous solutions. They exhibit similar transient spectral features (2 ps solvation dynamics and longer excited-state lifetime), so that there are no new dynamical processes evident in aqueous solution even if part of the signal were due to dimers. There are other reported cases in which no evidence was found for aggregates in temporal measurements on bulk samples where aggregates are known to be present. While static absorption spectra show that oxazine dye aggregates are present even in dilute solutions, the time-resolved experiments of Anfinrud et al. did not indicate any contribution from CV aggregates.<sup>17</sup> Similarly, in the measurements by Kamat and co-workers on aqueous solutions of CV, there is no evidence of a time-dependent signal from aggregates without the addition of silica and tin oxide colloids.<sup>1,4</sup>

**SHG Results.** For the single-color TSHG measurements the laser wavelengths were set near the dimer absorption maximum (570–600 nm). The experiments were carried out on concentrated ( $1\text{--}3 \times 10^{-4}$  M) aqueous solutions of NB, CV, and OX720 containing a small amount of LiCl. For NB, the SHG signal was large enough to measure TSHG signals without the addition of salt as well. In all cases, the pump pulse resulted in a decreased SHG signal. TSHG curves are given in Figure 2 for NB, CV, and OX720 aqueous/LiCl solutions and for aqueous NB without salt. All the responses are characterized by an instrument-limited decrease in SHG signal intensity followed by a partial recovery well described by a biexponential decay convoluted with the instrument function. Fitting the curves yields similar results for all three dyes with a short decay time,  $\tau_1 = 4\text{--}5$  ps, a longer decay time,  $\tau_2 = 20\text{--}30$  ps, and a long time ( $>50$  ps), persistent component. The relative amplitudes are typically 55%, 40%, and 5% of the total transient signal, respectively. For NB without salt,  $\tau_1 = 8$  ps and  $\tau_2 = 44$  ps. The derived constants are given in Table 1.



**TABLE 1: Decay Times for Transient Response of Surface TSHG of Aqueous Oxazine Dye Solutions**

dye	$\tau_1/\text{ps}^a$	$\tau_2/\text{ps}^a$	remaining <sup>a</sup>
oxazine 720	5 (57%)	23 (41%)	2%
cresyl violet	4 (64%)	23 (24%)	12%
Nile blue	5 (37%)	22 (55%)	8%
Nile blue w/o LiCl	8 (62%)	44 (38%)	<1%

<sup>a</sup> The uncertainty in the lifetimes and fractions remaining based on the nonlinear fitting procedure is  $\pm 15\%$ .

In our detection scheme, we directly measure the change of SHG intensity induced by the pump pulse as a function of time,  $\Delta I(t)$ , by chopping the pump beam and using lock-in detection. The resultant electric field,  $E(t) \propto \sqrt{I_{\text{SHG}}(t)}$ , rather than intensity,  $I(t)$ , is rigorously linear with population (or more generally,  $\chi^{(2)}$ , as described below). But, if the signal depends on the population of only one state (the ground state in the present case) and for low levels of excitation,  $\Delta I(t) \propto \Delta N(t)$  is a close approximation. The population as a function of time can be written  $N(t) = N_0 + \Delta N(t)$ , and the SHG signal intensity,  $I(t)$ , is given by  $I(t) = I_0 + \Delta I(t) \propto (N_0 + \Delta N(t))^2 = N_0^2 + \Delta N(t)(2N_0 + \Delta N(t)) \approx N_0^2 + 2\Delta N(t)N_0$ . Therefore, for low levels of excitation or small values of  $\Delta N/2N$ , the time dependence of the intensity reasonably approximates population changes, i.e.,  $\Delta I(t) \propto \Delta N(t)$ . We analyzed several data sets (including those shown in Figure 2, for which  $\Delta N/N < 0.1$ ) using the field amplitude as well as  $\Delta I(t)$ , and the resulting decay times were the same within our experimental uncertainty.

## Discussion

The TSHG signal recovery we observe is interpreted as GSR of dimers. In our previous study<sup>28</sup> we demonstrated that the SHG signal originates from dimers and that their concentration is high at the air/water interface of aqueous dye solutions. The steady-state SHG signals observed were attributed to dimers based on the SHG spectra, which indicate a single band, and the SHG dependence on solution composition. The SHG signal intensity correlates with conditions that favor aggregation in bulk solutions. No SHG was detected from the interface of methanolic solutions or from other oxazines in aqueous solution for which negligible aggregation occurs in the bulk. It was also found that SHG is enhanced by adding salt, which is known to promote dimer formation in the bulk.<sup>32</sup>

The pump pulse excites dye molecules to the first excited state via the  $S_0 \rightarrow S_1$  transition. The subsequent SHG time dependence could in principle be due to changes in population (in the ground or excited states or both), orientation, or resonance effects (such as excited-state dynamics). Various possible mechanisms are considered in terms of the dimer energy levels, which are depicted in Figure 3. Since it appears that the SHG probe is one-photon resonant with the  $S_0 \rightarrow S_1$  transition of the aggregate, we attribute the SHG recovery to GSR. The generated SHG electric field at the frequency  $2\omega$ ,  $E(2\omega)$ , is proportional to the square root of the measured SHG intensity ( $E(2\omega) \propto \sqrt{I_{\text{SHG}}(2\omega)}$ ). The generated field ( $E_I(2\omega)$ , where the field subscript refers to polarization direction) depends on the incident fields ( $E_J(\omega)$  and  $E_K(\omega)$ , both of which are provided by the same beam in our case) and the second-order molecular susceptibility,  $\chi_{IJK}^{(2)}$ .

$$E_I(2\omega) \propto \chi_{IJK}^{(2)} E_J(\omega) E_K(\omega) \quad (1)$$

In the absence of the pump pulse (for  $t < 0$ ), the SHG depends only on the ground-state susceptibility, which can be written in

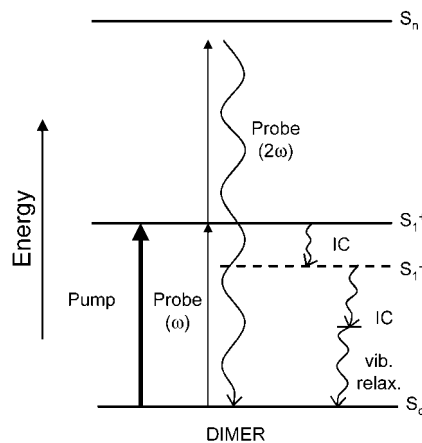


**Figure 3.** Schematic energy level diagram for an H-type aggregate. See text for discussion and for label definitions.

terms of the ground-state population,  $N_g$ , and molecular hyperpolarizabilities,  $\beta_{ijk}$ :<sup>33</sup>

$$\chi_{IJK}^{(2)} \propto N_g \sum_{ijk} \langle T_{IJKijk}(\theta, \phi, \delta) \rangle \beta_{ijk} \quad (2)$$

where  $T_{IJKijk}(\theta, \phi, \delta)$  is the transformation matrix between molecular ( $ijk$ ) and laboratory ( $IJK$ ) frames. The brackets denote the orientational ensemble average. After the excitation pulse transfers population from the ground state to the excited state (for  $t \geq 0$ ), the SHG signal can have contributions from both ground,  $\chi_g^{(2)}(t)$ , and excited state,  $\chi_{ex}^{(2)}(t)$ , susceptibilities. These can be affected by changes in the population ( $N_g(t)$  and  $N_{ex}(t)$ , as in ground-state recovery<sup>18–20</sup> and excited-state relaxation), the orientation ( $T_{IJKijk}(\theta, \phi, \delta)$ , as with rotation<sup>9,11,13</sup>), and resonance or spectral characteristics ( $\beta_{ijk}$ , as with time-dependent Stokes shifts due to solvation dynamics<sup>12</sup>). If the probe SHG ground-state hyperpolarizability,  $\beta_g$ , is dominated by the one-photon resonance via the  $S_0 \rightarrow S_1$  transition and it is much larger than the excited-state hyperpolarizability,  $\beta_g > \beta_e$ , then the signals will reflect the ground-state population (and/or orientation). There are several reasons to expect this to be true in our case.  $\beta_e$  resonances (either for  $\omega$  or  $2\omega$ ) must originate in  $S_1$  and terminate in a higher electronic state. We infer that the  $S_1 \rightarrow S_n$  and  $S_0 \rightarrow S_2$  resonances contribute less to  $\beta_g$  than the  $S_1 \rightarrow S_2$  since we found a much stronger correlation between the SHG spectra and the absorption spectrum at  $\omega$  than for the one at  $2\omega$ . Also, in the bulk TA/TG measurements we observe gain for single-color conditions near 600 nm, which indicates that the  $S_0 \rightarrow S_1$  transition moment is higher than for the  $S_1 \rightarrow S_2$  transition moment. Therefore, at least for the one-photon resonance from  $S_0$  and  $S_1$ ,  $\beta_g > \beta_e$ . The SHG recovery is nearly complete (>90%), and this provides further evidence that the signals are due to GSR. For a two-photon resonant SHG probe, the decay from the excited state accounts for <50% of the original transient.<sup>12</sup> Excited-state solvation dynamics or a dynamic Stokes shift cannot be invoked in our case, at least not for a large fraction of the signal, since we observe that most of the initial SHG decrease recovers. Consequently, the signals are attributed to population changes and GSR. TA/TG (e.g., of the bulk solutions) in this respect is more similar to two-photon resonant SHG (than to one-photon resonant) since it is sensitive to relative population changes for both the ground and excited states.

GSR has been observed previously when the probe pulse was one-photon resonant with the  $S_0 \rightarrow S_1$  transition, such as in studies by Meech and co-workers on R6G, MG,<sup>18,19</sup> and R110,<sup>20</sup>

and by Eisenthal and co-workers on MG and 3,3'-diethyloxadicyanocyanine iodide (DODCI)<sup>10</sup> and on R6G.<sup>9</sup> In contrast, probing via a two-photon resonance provides more symmetry between the ground and excited states so that the dynamics of the latter can be investigated. Zimdars et al. reported such a study of the solvation dynamics of coumarin 314 (C314) at the air/water interface.<sup>12</sup>

The fact that the SHG signal arises only from dimers in the ground state limits the possible assignments of the two recovery times measured. Possible interpretations for the SHG recovery include vibrational relaxation, rotational reorientation/diffusion, and IC/intersystem crossing (ISC) from the  $S_1/T_1$  excited states. Two independent, parallel mechanisms are required to account for the observed biexponential form of the transients. While the SHG recovery could result from either population or orientational changes, there is no indication of the latter. We do not observe an effect due to either the pump or probe polarization, suggesting that the SHG recovery is not due to orientationally dependent dynamics or affected by rotational motion, respectively. The SHG polarization dependence for the air/water interface of these solutions was investigated in our previous study.<sup>28</sup> The dye aggregates were found to be oriented at an angle  $\theta = 12\text{--}26^\circ$  for the  $z$ -axis with respect to the surface, assuming narrow angular distributions for  $\theta$  and  $\delta$ , where  $\delta$  is the rotation about the  $z$ -axis. Therefore the two observed lifetimes could result from the pump beam exciting two different orientationally dependent components, e.g., a bimodal angular distribution. Orientationally dependent solvation times were observed by Zimdars et al.<sup>11</sup> They found two separate solvation times depending on the polarization of the pump beam,  $820 \pm 60$  fs for  $s$ -pumped light and  $1215 \pm 90$  fs for  $p$ -pumped light for C314 at the air/water interface. These times were attributed to light being absorbed by molecules with transition moments aligned out-of-plane with respect to the interface for  $p$ -polarized light and in-plane for  $s$ -polarized light. We used a similar approach to investigate the possibility of orientationally dependent dynamics by measuring TSHG signals for different pump polarizations. No difference was found between  $p$ -polarized and  $s$ -polarized excitation in the recovery times. If the times measured were due to exciting molecules with different orientations and there were an orientational dependence on the decay times, varying the pump polarization would have a measurable effect on the observed times or the relative intensities of the two components.

Another orientational effect on the dynamics is molecular rotation, which can be detected by the polarization dependence of the SHG probe. Rotational reorientation dynamics have been measured for eosin B<sup>13</sup> and R6G<sup>9</sup> at air/water interfaces. We were unable to observe a significant increase in the weak signal detected for  $s$ -polarized SHG with  $45^\circ$  incident probe polarization ( $I_{s,45} < 0.05 I_{pp}$ ), which would have indicated an orientational component to the time dependence of the TSHG signal. The measured SHG recovery times are probably too short to be rotational times for the dimers. Rotational diffusion times for other dyes at liquid/solid interfaces and in aqueous solutions are on the order of 100–250 ps. For RB, Clarke et al.<sup>14</sup> measured rotational diffusion times for both the monomer and the H-aggregate dimer, which were found to be 250 ps and  $> 100$  ps, respectively. For aqueous solutions of NB, Habuchi et al.<sup>34</sup> measured the rotational anisotropy in the fluorescence emission from the dye monomer and deduced a rotational diffusion time of 110 ps in good agreement with the existing literature.<sup>31,35</sup> The dimer diffusion time was not determined exactly due to the experimental uncertainty in the measurements made. Zimdars

et al.<sup>36</sup> also measured the rotational diffusion of C314 at the air/water interface in an experimental arrangement similar to their study of solvation dynamics. Rotational times of 350 and 600 ps for out-of-plane and in-plane excitation were reported along with a 4.5 ns GSR time. These times are considerably longer than the time constants we observe, ruling out the possibility of rotational reorientation. Since we found no evidence for orientational effects on the signal as a result of investigating the polarization dependencies for the pump and probe, we conclude that the transient SHG signal reflects population changes.

Two parallel mechanisms for repopulating the ground state are required to account for the observed biexponential form of the transients. The shorter SHG recovery time could be due to ground state solvent relaxation after rapid IC. In their study of excited-state solvation dynamics of a monomeric dye at the air/water interface, Zimdars et al.<sup>12</sup> found behavior that was similar to the bulk solvation dynamics. The present case is not directly comparable because we may be looking at solvation relaxation of ground-state aggregates. Other possible mechanisms leading to GSR are IC and ISC.

The first step is to depopulate the  $S_1^+$  state via rapid IC. The rate of IC from the  $S_1^+$  excited state to the  $S_1^-$  state in H-aggregates has not been reported in the literature and it is assumed to be fast (sub-ps). A resolvable  $S_1^+ \rightarrow S_1^-$  IC should not be ruled out based on existing experimental evidence. In their fluorescence quantum yield measurements, Anfinrud et al.<sup>17</sup> did not detect any aggregate fluorescence, but based on the calculated quantum yield and the minimum fluorescence detection limit of their experiment the possibility should not be excluded.

The most probable explanations for the longer time SHG recovery are IC and ISC processes. Aggregate molecules returning to the ground state after excitation (and IC) will probably have excess internal energy and could relax on these time scales as discussed by Khairutdinov and Serpone.<sup>15</sup> Therefore vibrational relaxation of "hot" ground-state aggregates could account for the longer measured recovery time. IC/ISC from the  $S_1^-/T_1$  states to the ground state,  $S_0$ , has been proposed by Kamat and co-workers<sup>1–5</sup> and Nasr and Hotchandani<sup>6</sup> as the main relaxation route back to the ground state for aggregates on semiconductor particles. In their studies of oxazine dyes (CV<sup>1,4</sup> and NB<sup>6</sup>) at water/SiO<sub>2</sub> and water/SnO<sub>2</sub> interfaces, they report a single-exponential decay on SiO<sub>2</sub> and a biexponential decay on SnO<sub>2</sub> with decay times in the range 2–250 ps. (The second decay on SnO<sub>2</sub> is due to back electron transfer.) Our results are similar in that the observed dynamics are different for interfacial dimers than for what is seen for dyes in bulk solution. However, they find a single-exponential decay (for the dielectric or the semiconductor not considering the electron-transfer mechanism) while we find a biexponential recovery. They attribute the decay to an IC process,  $S_1/T_1 \rightarrow S_0$ , of the aggregate. In these studies and others, the lifetime of the  $S_1^+$ , the upper energy level of the excited-state H-aggregate, has been considered to be sub-ps due to IC to the  $S_1^-$  level. We cannot assign either of the recoveries to IC of the  $S_1^+$  to  $S_1^-$  energy level since both observed decays are due to GSR. It is surprising that we find more complicated dynamics at the air/water interface than in the studies at water/solid interfaces. The bulk nonaqueous phase in our experiment (air) is less perturbative and we are detecting only ground-state dynamics, whereas the other studies are sensitive to both ground and excited-state dynamics with TA/TG.

## Summary

This study represents one of the first studies of dye aggregate dynamics at the air/water interface. TSHG studies are presented for aqueous solutions of the oxazine dyes NB, CV, and OX720. The SHG signals previously have been shown to be due almost exclusively to dye dimers at the air/water interface. The SHG signal is lower after the pump pulse and it recovers biexponentially (with time constants of about 5 and 25 ps). The results for dyes at the interface are different than those observed for bulk dye solutions. Transient absorption/gain studies of the bulk dye solutions in water and methanol were also conducted, and the results can readily be explained in terms of the well-known mechanisms of solvation dynamics ( $\tau \sim 2$  ps) and excited-state lifetimes ( $\tau > 400$  ps). The SHG recovery is assigned to population changes since we found no evidence of orientational effects. The decay times are also probably too short to be due to rotational reorientation. Since the fundamental wavelength from which the SHG probe is generated appears to be one-photon resonant with the dye aggregate  $S_1 \rightarrow S_0$  transition, the recoveries are attributed to GSR and this severely restricts the possible explanations for the decay times observed. Two parallel mechanisms for repopulating the ground state are required to account for the observed biexponential form of the transients. Probably both IC and ISC processes are involved as intermediate steps in the SHG recovery. The shorter SHG decay time could be due to ground state solvent relaxation after rapid IC. Vibrational relaxation of "hot" aggregates after IC/ISC from the excited state is the most probable explanation for the longer time.

**Acknowledgment.** This work was supported by the Office of Naval Research through the Naval Research Laboratory. This work was performed while D.A.S. held a Naval Research Laboratory—National Research Council Research Associateship.

## References and Notes

- (1) Liu, D.; Kamat, P. V. *J. Chem. Phys.* **1996**, *105*, 965–970.
- (2) Nasr, C.; Liu, D.; Hotchandani, S.; Kamat, P. V. *J. Phys. Chem.* **1996**, *100*, 11054–11061.
- (3) Barazzouk, S.; Lee, H.; Hotchandani, S.; Kamat, P. V. *J. Phys. Chem. B* **2000**, *104*, 3616–3623.
- (4) Martini, I.; Hartland, G. V.; Kamat, P. V. *J. Phys. Chem. B* **1997**, *101*, 4826–4830.
- (5) Das, S.; Kamat, P. V. *J. Phys. Chem. B* **1999**, *103*, 209–215.
- (6) Nasr, C.; Hotchandani, S. *Chem. Mater.* **2000**, *12*, 1529–1535.
- (7) Yang, X.; Dai, Z.; Miura, A.; Tamai, N. *Chem. Phys. Lett.* **2001**, *334*, 257–264.
- (8) Eisensthal, K. B. *Annu. Rev. Phys. Chem.* **1992**, *43*, 627–661.
- (9) Eisensthal, K. B. *J. Phys. Chem.* **1996**, *100*, 12997–13006.
- (10) Eisensthal, K. B. *Chem. Rev.* **1996**, *96*, 1343–1360.
- (11) Castro, A.; Sitzmann, E. V.; Zhang, D.; Eisensthal, K. B. *J. Phys. Chem.* **1991**, *95*, 6752–6753.
- (12) Si, X.; Borguet, E.; Tarnovsky, A. N.; Eisensthal, K. B. *Chem. Phys.* **1996**, *205*, 167–178.
- (13) Zimdars, D.; Eisensthal, K. B. *J. Phys. Chem. A* **1999**, *103*, 10567–10570.
- (14) Zimdars, D.; Dadap, J. I.; Eisensthal, K. B.; Heinz, T. F. *Chem. Phys. Lett.* **1999**, *301*, 112–120.
- (15) Antoine, R.; Tamburello-Luca, A. A.; Hébert, Ph.; Brevet, P. F.; Girault, H. H. *Chem. Phys. Lett.* **1998**, *288*, 138–146.
- (16) Clark, J. B.; Smirl, A. L.; Van Stryland, E. W.; Mackey, H. J.; Russell, B. R. *Chem. Phys. Lett.* **1981**, *78*, 456–460.
- (17) Khairutdinov, R. F.; Serpone, N. *J. Phys. Chem. B* **1997**, *101*, 2602–2610.
- (18) Chen, S.-Y.; Horng, M.-L.; Quitevis, E. L. *J. Phys. Chem.* **1989**, *93*, 3683–3688.
- (19) Anfinrud, P.; Crackel, R. L.; Struve, W. S. *J. Phys. Chem.* **1984**, *88*, 5873–5882.
- (20) Meech, S. R.; Yoshihara, K. *Chem. Phys. Lett.* **1990**, *174*, 423–427.
- (21) Morgenthaler, M. J. E.; Meech, S. R. *Chem. Phys. Lett.* **1993**, *202*, 57–64.
- (22) Morgenthaler, M. J. E.; Meech, S. R. *J. Phys. Chem.* **1996**, *101*, 3323–3329.
- (23) Levinger, N. E.; Kung, K. Y.; Luther, B. M.; Willard, D. M. Absorption spectroscopy at liquid interfaces by resonant surface second harmonic generation, in *Laser Techniques for Surface Science II*; Hicks, J. M., Ho, W., Dai, H.-L., Eds.; *Proc. SPIE* **1995**, *2547*, 400–410.
- (24) Rabinowitch, E.; Epstein, L. F. *J. Am. Chem. Soc.* **1941**, *63*, 69–78.
- (25) McRae, E. G.; Kasha, M. *J. Chem. Phys.* **1958**, *28*, 721–722.
- (26) McRae, E. G.; Kasha, M. *Physical Processes in Radiation Biology*; Augenstein, L., Mason, R., Rosenberg, B., Eds.; Academic Press: New York, 1964; p 23.
- (27) Kasha, M.; Rawls, H. R.; El-Bayoumi, M. A. *Pure Appl. Chem.* **1965**, *11*, 371–392.
- (28) Isak, S. J.; Eyring, E. M. *J. Phys. Chem.* **1992**, *96*, 1738–1742.
- (29) Wachtveitl, J.; Huber, R.; Spörlein, S.; Moser, J. E.; Grätzel, M. *Int. J. Photoenergy* **1999**, *1*, 153–155.
- (30) Steinhurst, D. A.; Owrutsky, J. C. *J. Phys. Chem. B* **2001**, *105*, 3062–3072.
- (31) Owrutsky, J. C.; Baranavski, A. P. *J. Chem. Phys.* **1999**, *110*, 11206–11213.
- (32) Jarzęba, W.; Walker, G. C.; Johnson, A. E.; Kahlow, M. A.; Barbara, P. F. *J. Phys. Chem.* **1988**, *92*, 7039–7041.
- (33) Grofcsik, A.; Kubinyi, M.; Jones, W. J. *J. Mol. Struct.* **1995**, *348*, 197–200.
- (34) Das, K.; Sarkar, N.; Das, S.; Datta, A.; Nath, D.; Bhattacharyya, K. *J. Chem. Soc., Faraday Trans.* **1996**, *92*, 4993–4996.
- (35) Heinz, T. F. *Nonlinear Surface Electromagnetic Phenomena*; Ponath, H.-E., Stegeman, G. L., Eds.; North-Holland: Dordrecht, 1991.
- (36) Habuchi, S.; Kim, H.-B.; Kitamura, N. *Anal. Chem.* **2001**, *73*, 366–372.
- (37) Dutt, G. B.; Doraiswamy, S.; Periasamy, N.; Venkataraman, B. *J. Chem. Phys.* **1990**, *93*, 8498–8513.
- (38) Zimdars, D.; Dadap, J. I.; Eisensthal, K. B.; Heinz, T. F. *J. Phys. Chem. B* **1999**, *103*, 3425–3433.